Ecological Modelling 361 (2017) 184–196

Contents lists available at ScienceDirect

Ecological Modelling

journal homepage: www.elsevier.com/locate/ecolmodel

Phytoplankton functional diversity increases ecosystem productivity and stability

S.M. Vallina [a,*], P. Cermeno [a], S. Dutkiewicz [b], M. Loreau [c], J.M. Montoya [c]

[a] Institute of Marine Sciences (CSIC), Barcelona, Catalonia, Spain
[b] Earth, Atmospheric and Planetary Sciences (MIT), Cambridge, USA
[c] Theoretical and Experimental Ecology Station (CNRS and Paul Sabatier University), Moulis, France

ARTICLE INFO

Article history:
Received 18 August 2016
Received in revised form 18 June 2017
Accepted 19 June 2017

Keywords:
Shannon entropy
Plankton foodwebs
Species-traits
Ecological selection
Ecosystem modelling

ABSTRACT

The effect of biodiversity on ecosystem functioning is one of the major questions of ecology. However, the role of phytoplankton functional diversity in ecosystem productivity and stability under fluctuating (i.e. non-equilibrium) environments remains largely unknown. Here we use a marine ecosystem model to study the effect of phytoplankton functional diversity on both ecosystem productivity and its stability for seasonally variable nutrient supply and temperature. Functional diversity ranges from low to high along these two environmental axes independently. Changes in diversity are obtained by varying the range of uptake strategies and thermal preferences of the species present in the community. Species can range from resource gleaners to opportunists, and from cold to warm thermal preferences. The phytoplankton communities self-assemble as a result of species selection by resource competition (nutrients) and environmental filtering (temperature). Both processes lead to species asynchrony but their effect on productivity and stability differ. We find that the diversity of temperature niches has a strong and direct positive effect on productivity and stability due to species complementarity, while the diversity of uptake strategies has a weak and indirect positive effect due to sampling probability. These results show that more functionally diverse phytoplankton communities lead to higher and more stable ecosystem productivity but the positive effect of biodiversity on ecosystem functioning depends critically on the type of environmental gradient.

1. Introduction

Biodiversity affects ecosystem functioning and services (Loreau et al., 2002; Duffy, 2009). The positive effect of species diversity on the production and temporal stability of terrestrial plant communities has been studied extensively both theoretically and empirically (Tilman et al., 1997, 2006; Naeem et al., 2012). The diversity of phytoplankton communities in natural freshwater and brackish habitats has been shown to increase ecosystem stability and resource use efficiency (Ptacnik et al., 2008). The role of marine phytoplankton diversity in oceanic ecosystem functioning and stability remains, however, largely unknown. The fact that plankton species inhabit an open fluid environment places some particular constrains to aquatic ecosystems that are absent in their terrestrial counterparts (Carr et al., 2003). In particular, the degree of resource competition is believed to be stronger in aquatic phytoplankton than in terrestrial plants because of the faster homogenization of nutrients (Hutchinson, 1961; Huston and DeAngelis, 1994). Early theoretical work suggests that under these conditions the diversity of planktonic species should be particularly low due to competitive exclusion, which begets foodweb instability (May, 1974; Sommer, 2002). However, these theoretical predictions are in open conflict with observations in field, which find a huge diversity of plankton species. This led to the Paradox of the Plankton (Hutchinson, 1961).

More recent ecological theory has been trying to reconcile this apparent contradiction between theory and field data (Loreau, 2010). While the focus of the previous theoretical framework was on individual population dynamics under steady-state conditions, the current approach places the focus on community- or ecosystem-level dynamics under non-equilibrium conditions. This new theoretical framework suggests that species diversity can increase aggregate community-level properties such as total primary production or biomass (Loreau, 2010). Different species may have distinct ecological niches and thus would respond differently to environmental changes, leading to an asynchrony of individual population dynamics (Loreau and de Mazancourt, 2013). Species dynamics are said to be “asynchronous” when their population

* Corresponding author.

http://dx.doi.org/10.1016/j.ecolmodel.2017.06.020

fluctuations in response to external environmental variability are not positively correlated among them (Loreau and de Mazancourt, 2013). Asynchronous responses should thus have a "buffering effect" on aggregate properties, leading to the insurance hypothesis of biodiversity (Yachi and Loreau, 1999), which has received considerable support from both theory and experimental manipulations of plant communities (Yachi and Loreau, 1999; Hector et al., 1999; Tilman et al., 2001, 2006).

Species diversity is also the basis for functional compensation, which may lead to the "enhancing effect" of biodiversity on ecosystem functioning through compensatory dynamics. When the species present in a community have complementary functional roles, this may be expected to increase total production (Loreau, 2010). Differences in fundamental niches may also lead to differences in their realized temporal niches (i.e. asynchrony of species through time). While temporal complementarity has been shown to increase ecosystem stability, its effect in the ecosystem's production capacity remains unclear (Loreau, 2010). However, for the marine environment, phytoplankton diversity may lead to higher primary productivity by maximizing resource use efficiency through transient population dynamics. The main mechanism is the competitive *selection* and *dominance* of the most efficient species through time, which can be seen as a form of temporal niche complementarity among species (Loreau, 2010).

In order to apply and formally evaluate the validity of these ideas for the marine environment, we have devised a 1D (depth-resolved) modelling framework of seasonal phytoplankton dynamics in which we manipulate the functional diversity of the species along two environmental gradients: dissolved inorganic nitrogen (DIN) and sea surface temperature (SST). The ecosystem has three trophic levels: photosynthetic phytoplankton, herbivorous zooplankton and carnivorous zooplankton. Only the diversity of phytoplankton species is resolved. Phytoplankton functional diversity varies by changing the species similarity (i.e. redundancy or niche overlapping) along these two environmental axes independently. Current ecological theory and terrestrial field data supports the insurance hypothesis of biodiversity for total plant biomass or production (Yachi and Loreau, 1999; Hector et al., 1999; Tilman et al., 2001, 2006). Here we evaluate the effect of phytoplankton functional diversity on annually-averaged community-level primary production (P) (mmol C m^{-3} d^{-1}) and its temporal variability (coefficient of variation; CV) over a seasonal cycle of nutrient supply and ocean temperature.

2. Functional diversity

The 16 phytoplankton species in our ecosystem model range from resource gleaners to opportunists, and from cold to warm thermal preferences. Resource gleaners are slow-growing species that have high uptake affinity and thus are more competitive under low nutrient concentrations. Resource opportunists are fast-growing species that have a lower uptake affinity and thus are more competitive under high nutrient concentrations (Grover, 1997). Each nutrient uptake strategy leads to a different nutrient concentration optima (N_{opt}) through *resource competition*, while each different thermal preference leads to a different temperature optima (T_{opt}) for growth under *environmental filtering*. Changes in functional diversity are driven by the range of uptake strategies and thermal preferences of the species present in the community. The potential functional diversity of a community in the absence of species interactions can be measured as the Euclidean distance (see Section 3) of the two species traits that determine the nutrient uptake strategy and the temperature preference, which are the maximum growth rate (μ_{max}) and the temperature optima (Fig. 1). The realized functional diversity of a community after species interactions can be measured as the *continuous* entropy of the probability density distribution of the species (see Methods). For either measure, the diversity in uptake strategies is determined by the spread of μ_{max} values of the species present in each community. A higher spread of μ_{max} values implies a higher spread of the contrasting gleaner-opportunist strategies and thus a larger spread of the different N_{opt} values. Likewise, the diversity in thermal preferences is determined by the spread of T_{opt} values of the species present in each community. There are four temperature preferences per uptake strategy. We obtained 64 phytoplankton communities of different functional diversity by increasing the spread of both μ_{max} (8 levels) and T_{opt} (8 levels) independently. We then compute the annually averaged total primary production and its temporal variability (coefficient of variation) for each degree of functional diversity.

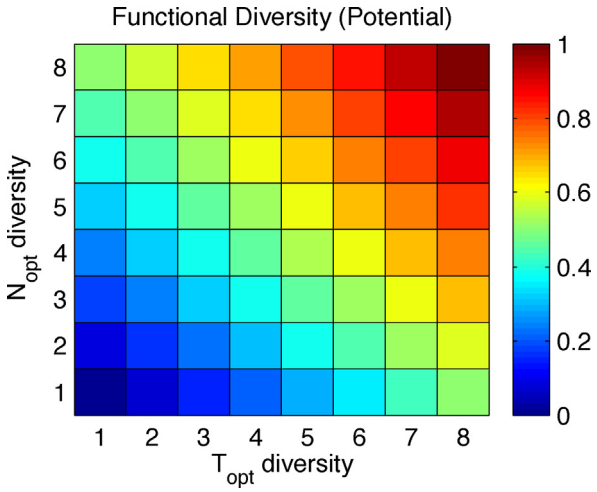

Fig. 1. Functional diversity measured as the Euclidean distance of the species optimal nutrient concentration (N_{opt}) and optimal temperature (T_{opt}) of the phytoplankton community. The vertical axis gives the level of diversity in uptake strategies, which is determined by the spread of N_{opt} values of the species present in each community. The horizontal axis gives the level of diversity in thermal preferences, which is determined by the spread of T_{opt} values of the species present in each community. The different uptake strategies arise from a "gleaner-opportunist" trade-off between nutrient uptake affinity (θ) and maximum growth rate ($\theta \cdot \mu_{max}$ = constant). Slow-growing gleaners are superior competitors at low N_{opt} due to their higher affinity. Fast-growing opportunists are superior competitors at high N_{opt} due to their higher maximum growth rate. N_{opt} is directly related to μ_{max}. The level of functional diversity was increased sequentially (8 steps) along each axis independently by gradually increasing the spread of μ_{max} and T_{opt} values of each community. The species richness is always 16 for all the $8 \times 8 = 64$ functional diversity levels, what varies is the degree of functional similarity of each phytoplankton community. The highest diversity at square (8, 8) represents a functionally diverse phytoplankton community with four uptake strategies (from low N_{opt} gleaners to high N_{opt} opportunists) and four temperature preferences (from low T_{opt} to high T_{opt}) – i.e. all 16 species are ecologically distinct and very different. The lowest diversity at square (1, 1) represents a functionally redundant community with just one uptake strategy (after making all species converge to the same μ_{max}) and one temperature preference (after making all species converge to the same T_{opt}) – i.e. all 16 species are ecologically equivalent. All other 58 squares represent different communities with a level of functional diversity that lies between these two extreme cases – i.e. all 16 species are ecologically distinct but they can range from very similar at square (2, 2) to very different at square (7, 7). Highly diverse communities thus cover a larger range of uptake strategies and thermal preferences than less diverse communities.

The four uptake strategies and four temperature preferences lead to a community with $4 \times 4 = 16$ phytoplankton species (see Fig. 2 and Table S1 in Supplementary Material), each of them filling a particular ecological niche (N_{opt}, T_{opt}) when they are ecologically different. The resource uptake strategies arise from the assumed trade-off between the nutrient uptake affinity (θ) and maximum growth rate ($\theta \cdot \mu_{max}$ = constant), which leads to a quadratic relationship between the half-saturation constant for uptake and the maximum growth rate (Meyer et al., 2015) that make the uptake

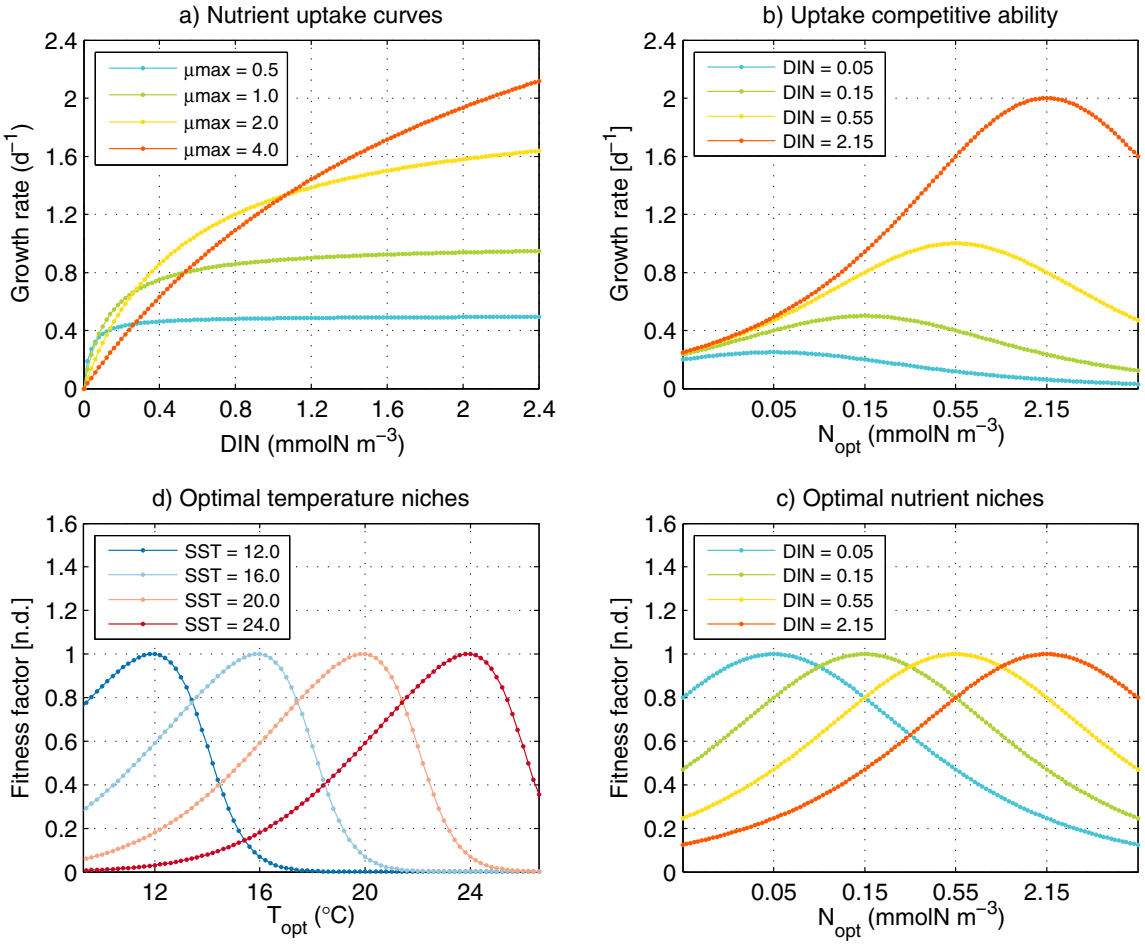

Fig. 2. Optimal niches of nutrient concentration (N_{opt}; mmol N m^{-3}) from gleaners to opportunists as a function of dissolved inorganic nitrogen DIN, and optimal niches of temperature (T_{opt}; °C) from colder to warmer preference as a function of sea surface temperature SST for the highest functional diversity phytoplankton community. (a) The resource uptake [d^{-1}] curves of the four uptake strategies result from a trade-off between uptake affinity and maximum growth rate ($\theta \cdot \mu_{max}$ = constant): slow-growing gleaners are superior competitors at low nutrient concentration because they have a higher nutrient affinity, while fast-growing opportunists are superior competitors at high nutrient concentration because they have a higher maximum growth rate. Thus each μ_{max} corresponds to a different N_{opt}. (b) The competitive fitness d^{-1} of the uptake strategies depends on the nutrient concentration (e.g. when DIN = 0.05 mmol N m^{-3} the fastest uptake corresponds to nutrient gleaners; when DIN = 2.15 mmol N m^{-3} the fastest uptake corresponds to nutrient opportunists). (c) The fitness factor [n.d.] (i.e. competitive fitness normalized by its maximum value) reveals more clearly the nutrient niches as a function of the resource uptake strategy. (d) The fitness factor [n.d.] of the thermal niches depends on the ocean temperature. A total of four optimal uptake strategies (c) and four optimal temperature preferences (d) lead to a combination of $4 \times 4 = 16$ ecological niches (N_{opt}, T_{opt}), each of them filled by one of the 16 phytoplankton species present in the community.

curves to intersect (Sommer, 1986; Grover, 1997). For this growth-affinity or "gleaner-opportunist" trade-off (Grover, 1997; Litchman et al., 2015), the optimal nutrient concentration of each species corresponds to their half-saturation constant for nutrient uptake, unless all species have exactly the same uptake strategy because then the very concept of N_{opt} vanishes. Therefore, μ_{max} alone determines the nutrient uptake curve and thus the N_{opt} (see Fig. 2). A gleaner-opportunist trade-off has been suggested to explain the observed succession of phytoplankton species in natural communities (Sommer, 1981; Smayda and Reynolds, 2001), and has been confirmed in the laboratory using chemostat competition experiments where the gleaner wins under steady-state nutrient supply and the opportunist wins under pulsed nutrient supply (Sommer, 1984, 1985, 1986; Cermeno et al., 2011). When placed together, a continuum of these resource uptake strategies leads to different nutrient niches from low to high concentration through resource competition (see Fig. 2c). Similarly, a continuum of thermal optima leads to different temperature niches under environmental filtering (see Fig. 2d).

Decreasing the level of functional diversity of the phytoplankton community means increasing the similarity of the species until they all become perfectly redundant (Thebault and Loreau, 2005). For the highest diversity there is only one possible set of phytoplankton species that can fill all the 16 (N_{opt}, T_{opt}) niches, one per species (see Table S1 in Supplementary Material). At the other extreme, however there are 16 possible combinations of phytoplankton species for the lowest functional diversity, each corresponding to one of the 16 (N_{opt}, T_{opt}) ecological niches to where all the species in the community can functionally converge (see Table S2 in Supplementary Material). Since we change functional diversity in 8 incremental steps along each environmental axis independently (see Fig. 1), this led to a total of: $8 \times 8 \times 16 = 1024$ individual simulations that were performed to cover the whole range of community combinations (see Figs. S3 and S4).

The interplay of competition and filtering leads to asynchrony by confining species to their particular nutrient and thermal niches. However, nutrient optima differ from temperature optima in which they only appear when different nutrient uptake strategies are present together in the same phytoplankton community; otherwise when just one uptake strategy is present, there are no N_{opt} niches as such. That means that when all species are ecologically equivalent in their uptake strategy, resource competition is neu-

Table 1
Ecosystem model state-variables.

Variable	Description	Units
P_j	Phytoplankton species j	mmol N m^{-3}
Z_1	Zooplankton herbivore	mmol N m^{-3}
Z_2	Zooplankton carnivore	mmol N m^{-3}
NO_3	Nitrates	mmol N m^{-3}
NH_4	Ammonium	mmol N m^{-3}
DON	Dissolved organic nitrogen	mmol N m^{-3}
PON	Particulate organic nitrogen	mmol N m^{-3}

tral. Under these conditions any one single uptake strategy can freely occupy the whole range of nutrient concentrations. This is because the species *fundamental niche* (Hutchinson, 1957) for nutrients is given by their resource uptake curves, which are open-ended to the right (i.e. high nutrient concentrations are not harmful for growth; see Fig. 2a). Therefore all species share and could potentially grow over the whole range of nutrient concentration that is above its basal requirements. Only when species with different uptake strategies are placed together, will the species be pushed to their particular optima of nutrient concentration where they are the best competitors, that is, to their *realized niche* (Hutchinson, 1957). However, it is worth mentioning that solar radiation is also a growth-limiting resource, although here assumed to be affecting equally all species. Therefore, there is an implicit potential resource-ratio differentiation among species. Thermal optima, on the other hand, are intrinsic properties that do not depend on the other species T_{opt}. The thermal fundamental niche of species is given by their $T_{opt} \pm$ a tolerance range above or below which the species cannot grow. This leads to distinct closed-ended negative-skew Gaussian bell curves, regardless of who else is present in the community. Higher diversity of temperature preferences may narrow the thermal realized niches of each species but will at the same time increase the coverage of the temperature gradient by the whole phytoplankton community. When only one thermal preference is present in the community, large segments of the temperature gradient will be devoid of any phytoplankton species (Isbell et al., 2017). This distinction between *shared* (open-ended) fundamental niches for nutrients and *distinct* (closed-ended) fundamental niches for temperature (Wisheu, 1998) is important to understand their effect on ecosystem functioning.

3. Methods

3.1. MIT ecological selection model (MITesm)

The ecosystem model (see Appendix A) is a version of the MIT ecological selection model (Vallina et al., 2014a) forced using a 1D (depth-resolved) physical framework setup. Biotic organisms and abiotic compartments are passively mixed in the column water by vertical turbulent diffusion (see Fig. 3). Only detritus is subject to vertical sinking. The foodweb complexity is modular since we can select any number of species per trophic level. There are three trophic levels: photo-autotrophic phytoplankton, herbivorous zooplankton and carnivorous zooplankton. The model state variables are given in Table 1, the model terms are given in Table 2, and the model parameters are given in Table 3. The rate of change of the modelled phytoplankton (Eq. (1)) and zooplankton populations (Eq. (2)) results from the balance between gross production (Eqs. (12) and (31)), exudation (Eqs. (34) and (35)), constant mortality (Eqs. (38) and (39)), and turbulent diffusion. Phytoplankton production (Eq. (12)) is a function of nutrient limitation (Eq. (13)), photosynthetic active radiation (PAR) limitation (Eq. (16)) and temperature dependence (Eq. (17)). Zooplankton production (Eq. (31)) is a function of prey limitation (Eq. (27)) without temperature dependence. For this work we have selected a configuration with

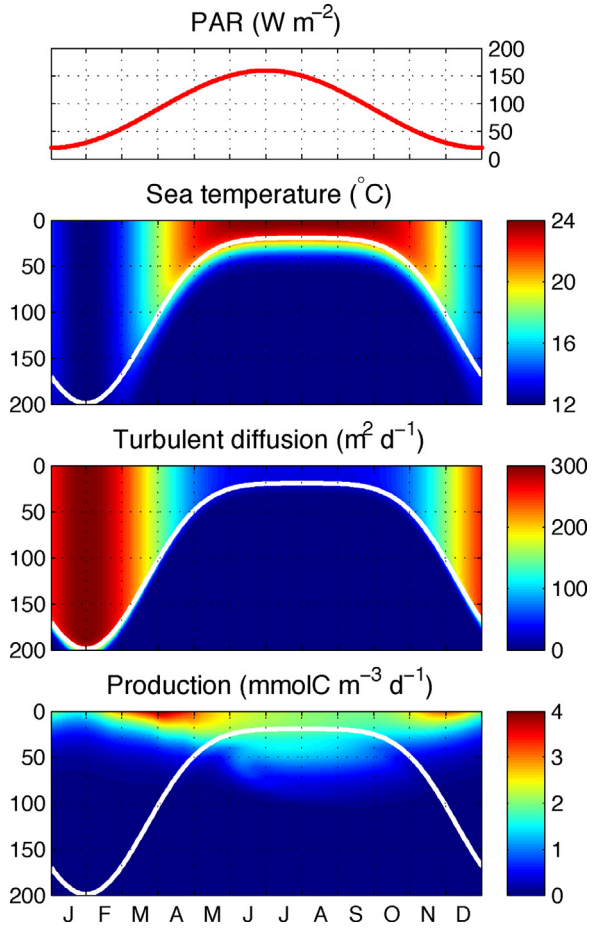

Fig. 3. Seasonal environmental forcing of photosynthetically active radiation (top panel), ocean temperature (middle-top panel), turbulent diffusivity (middle-bottom panel), and seasonal variability of community-level primary production (bottom-panel) for the highest functional diversity phytoplankton community. The vertical axis represent depth [m]. The white continuous line gives the depth of the mixing layer. The winter turbulent mixing brings nutrients to the ocean surface that are taken up by the phytoplankton community during the spring bloom when solar radiation is increasing and the mixing layer depth is decreasing (Behrenfeld and Boss, 2014). Production decreases over summer due to nutrient exhaustion after vertical sinking of senescent phytoplankton cells as detritus. The secondary autumn bloom in production results from the deepening of the mixing layer that brings nutrients to the surface when solar radiation is decreasing but still high enough to sustain production.

Table 2
Ecosystem model terms.

Term	Description	Units
F_P	Production of phytoplankton	mmol N m^{-3} d^{-1}
$F_P^{NO_3}$	Production of phytoplankton on nitrate	mmol N m^{-3} d^{-1}
$F_P^{NH_4}$	Production of phytoplankton on ammonium	mmol N m^{-3} d^{-1}
F_Z	Production of zooplankton	mmol N m^{-3} d^{-1}
E_P	Excretion of phytoplankton	mmol N m^{-3} d^{-1}
E_Z	Excretion of zooplankton	mmol N m^{-3} d^{-1}
G_P	Grazing on phytoplankton	mmol N m^{-3} d^{-1}
G_Z	Grazing on zooplankton	mmol N m^{-3} d^{-1}
M_P	Mortality of phytoplankton	mmol N m^{-3} d^{-1}
M_Z	Mortality of zooplankton	mmol N m^{-3} d^{-1}
M_{NH_4}	Decomposition of ammonium	mmol N m^{-3} d^{-1}
M_{DON}	Decomposition of dissolved organic nitrogen	mmol N m^{-3} d^{-1}
M_{PON}	Decomposition of particulate organic nitrogen	mmol N m^{-3} d^{-1}

16 phytoplankton species, 2 zooplankton species (one generic herbivore being fed upon by one top carnivore) and without bacteria; recycling of nutrients assumes linear constant degradation rates (see Eqs. (40)–(42)). The generic herbivore zooplankton feeds upon

Table 3
Ecosystem model parameters.

Parameter	Symbol	Value	Units	
Phytoplankton	Maximum specific growth rate	$\mu_{P_j}^{max}$	0.5–4.0	d^{-1}
Phytoplankton	Half-saturation for DIN uptake	K_{P_j}	0.05–2.15	mmol N m^{-3}
Phytoplankton	Optimal temperature	$T_{opt}^{P_j}$	12.0–24.0	°C
Phytoplankton	Optimal irradiance	I_{opt}	120	W m^{-2}
Phytoplankton	Temperature tolerance	σ_T	4.0	°C
Phytoplankton	Gaussian skewness	ρ_T	4.0	n.d.
Phytoplankton	Assimilation efficiency	β_P	0.8	n.d.
Phytoplankton	Mortality specific rate	ψ_P	0.05	d^{-1}
Phytoplankton	Excretion fraction going to NO_3	$\varepsilon_{(P\rightarrow NO_3)}$	1/4	n.d.
Phytoplankton	Excretion fraction going to NH_4	$\varepsilon_{(P\rightarrow NH_4)}$	1/4	n.d.
Phytoplankton	Excretion fraction going to DON	$\varepsilon_{(P\rightarrow DON)}$	1/4	n.d.
Phytoplankton	Excretion fraction going to PON	$\varepsilon_{(P\rightarrow PON)}$	1/4	n.d.
Phytoplankton	Mortality fraction going to NO_3	$\Omega_{(P\rightarrow NO_3)}$	1/4	n.d.
Phytoplankton	Mortality fraction going to NH_4	$\Omega_{(P\rightarrow NH_4)}$	1/4	n.d.
Phytoplankton	Mortality fraction going to DON	$\Omega_{(P\rightarrow DON)}$	1/4	n.d.
Phytoplankton	Mortality fraction going to PON	$\Omega_{(P\rightarrow PON)}$	1/4	n.d.
Zooplankton	Herbivore preference on phytoplankton *i*	ϕ_{i1}	1	n.d.
Zooplankton	Carnivore preference on phytoplankton *i*	ϕ_{i2}	0	n.d.
Zooplankton	Herbivore preference on zooplankton *i*	φ_{i1}	0	n.d.
Zooplankton	Carnivore preference on zooplankton *i*	φ_{i2}	1	n.d.
Zooplankton	Maximum specific growth rate	$\mu_{Z_j}^{max}$	1.0	d^{-1}
Zooplankton	Half-saturation for grazing	K_{Z_j}	1.0	mmol N m^{-3}
Zooplankton	Killing-the-winner parameter	α	2.0	n.d.
Zooplankton	Grazing Hill coefficient	β	2.0	n.d.
Zooplankton	Assimilation efficiency	β_Z	0.4	n.d.
Zooplankton	Mortality specific rate	ψ_Z	0.05	d^{-1}
Zooplankton	Excretion fraction going to NO_3	$\varepsilon_{(Z\rightarrow NO_3)}$	1/4	n.d.
Zooplankton	Excretion fraction going to NH_4	$\varepsilon_{(Z\rightarrow NH_4)}$	1/4	n.d.
Zooplankton	Excretion fraction going to DON	$\varepsilon_{(Z\rightarrow DON)}$	1/4	n.d.
Zooplankton	Excretion fraction going to PON	$\varepsilon_{(Z\rightarrow PON)}$	1/4	n.d.
Zooplankton	Mortality fraction going to NO_3	$\Omega_{(Z\rightarrow NO_3)}$	1/4	n.d.
Zooplankton	Mortality fraction going to NH_4	$\Omega_{(Z\rightarrow NH_4)}$	1/4	n.d.
Zooplankton	Mortality fraction going to DON	$\Omega_{(Z\rightarrow DON)}$	1/4	n.d.
Zooplankton	Mortality fraction going to PON	$\Omega_{(Z\rightarrow PON)}$	1/4	n.d.
NH_4	Decomposition specific rate	ψ_{NH_4}	0.1	d^{-1}
NH_4	Decomposition fraction going to NO_3	$\delta_{(NH_4\rightarrow NO_3)}$	1.0	n.d.
DON	Decomposition specific rate	ψ_{DON}	0.1	d^{-1}
DON	Decomposition fraction going to NO_3	$\delta_{(DON\rightarrow NO_3)}$	1/2	n.d.
DON	Decomposition fraction going to NH_4	$\delta_{(DON\rightarrow NH_4)}$	1/2	n.d.
PON	Decomposition specific rate	ψ_{PON}	0.1	d^{-1}
PON	Decomposition fraction going to NO_3	$\delta_{(PON\rightarrow NO_3)}$	1/3	n.d.
PON	Decomposition fraction going to NH_4	$\delta_{(PON\rightarrow NH_4)}$	1/3	n.d.
PON	Decomposition fraction going to DON	$\delta_{(PON\rightarrow DON)}$	1/3	n.d.
PON	Sinking rate	ω	1.0	m d^{-1}
PAR	Irradiance vertical attenuation due to water	k_w	0.04	m^{-1}
PAR	Irradiance vertical attenuation due to self-shading	k_p	0.02	m^2 mmol N^{-1}

all phytoplankton species with killing-the-winner (KTW) predation strategy (see Eq. (25), where parameter α >1 implies active prey-switching). The generic carnivore zooplankton feeds upon the herbivore zooplankton and upon itself acting as a closure term (see Eq. (26)) (Vallina et al., 2014b). The model mass currency is nitrogen and it resolves four types of abiotic compounds: nitrates (NO_3), ammonium (NH_4), dissolved organic nitrogen (DON) and particulate organic nitrogen (PON) (Eqs. (3)–(6); respectively). The model assumes Monod kinetics for the uptake of dissolved inorganic nitrogen (DIN = NO_3 + NH_4) and therefore uptake and growth are assumed to be coupled (Eqs. (14) and (15)). There is only one nutrient uptake affinity ($\theta_j = \mu_{P_j}^{max}/K_{P_j}$) for each species *j* which applies for both nitrate and ammonium. However, ammonium is assumed to be taken up preferentially over nitrate (Eqs. (15) and (14)) (Vallina and Le Quéré, 2008). Temperature preferences (Fig. 3) follow negative-skew gaussian bell curves (Eq. (17)) where T_{opt} defines the optimal temperature for growth and σ_T the temperature tolerance range (Eq. (22)). Solar radiation limitation follows a positive-skew non-gaussian bell curve (Eq. (16)) where I_{opt} defines the optimal irrandiance for growth, after which phytoplankton populations suffer photoinhibition. Solar irradiance is subjected to vertical exponential attenuation due to water absorption and phytoplankton self-shading (Eq. (23)). Light harvesting capabilities are common to all phytoplankton species and phytoplankton self-shading is also assumed to affect equally all species. Thus there is no differential fitness along the solar radiation environmental gradient. The coupled biophysical model was run for 4 years until reaching a repeated seasonal cycle of the population dynamics. The input data used as environmental variables for the model (i.e. solar irradiance, sea temperature, turbulence) were numerically generated to simulate a seasonal forcing characteristic of subtropical regions. The model is written in Matlab/Octave computer programming language.

3.2. Species-trait variability

Functional diversity refers to phytoplankton species-trait variability along two environmental gradients independently: dis-

solved nutrient concentration and ocean temperature. Regarding the uptake strategy, there is a transition from resource gleaners to resource opportunists. The diversity in nutrient uptake strategies results from a "gleaner-opportunist" trade-off that provides each phytoplankton species with a particular nutrient niche: slow-growing nutrient gleaners are superior competitors at low nutrient concentration because they have a higher nutrient affinity, while fast-growing nutrient opportunists are superior competitors at high nutrient concentration because they have a higher maximum growth rate (Litchman et al., 2015). This growth-affinity trade-off ($\theta \cdot \mu_{max}$ = constant) implies that the species-trait maximum growth (μ_{max}) alone is enough to define the nutrient uptake curve (see Fig. 2a) and thus the optimal nutrient concentration (N_{opt}) of any given uptake strategy (see Fig. 2d). The diversity in temperature preferences results from different temperature optima (T_{opt}) with a tolerance range (see Fig. 2c).

There are four N_{opt} and four T_{opt} (see Fig. 2) which leads to $4 \times 4 = 16$ species, each with a particular nutrient-temperature optimal niche when they are ecologically different. We decrease functional diversity in 8 steps along each axis (nutrient and temperature) independently until making all species converge to the same μ_{max} and T_{opt}, which leads to $8 \times 8 = 64$ functional diversity levels (see Fig. 1) for each final nutrient-temperature niche where all species become perfectly redundant (full niche overlapping). Therefore the variability of niches (16) and functional diversities (64) leads to a total of $16 \times 64 = 1024$ individual simulations. For each simulation we compute the functional diversity (potential and realized) of the annually-averaged phytoplankton community, the effective richness, the annually averaged community-level production (mmol C m^{-3} d^{-1}) and its temporal stability (i.e. inverse of the coefficient of variation) (see Figs. S3 and S4 in Supplementary Material). The potential functional diversity was measured as the euclidean distance $d = (\sqrt{\sum (x_j - \bar{x})^2} + \sqrt{\sum (y_j - \bar{y})^2})/2$ of the species-traits, where $x = N_{opt}$ (in log scale) and $y = T_{opt}$ (in linear scale) (see Fig. 1). Note that N_{opt} is directly related to μ_{max} and equal to the half-saturation constant for nutrient uptake K_P. The realized functional diversity was measured as the exponential of the differential (i.e. continuous) entropy (Shannon, 1948) $h = -\int\int f(x, y) \ln f(x, y) dx\, dy$ of the bivariate gaussian probability density function f(x,y) that was fitted to the observed species distribution of each annually-averaged phytoplankton community (see Fig. 6). The gaussian approximation is fairly accurate and leads to a good agreement between the observed and predicted biomass of each phytoplankton species (see Fig. S1). The effective richness was computed as the exponential of the Shannon (i.e. discrete) entropy (Shannon, 1948) $H = -\sum p_j \ln p_j$, where p_j is the proportion of species j in each annually-averaged phytoplankton community. The discrete (Shannon) entropy gives a measure of the richness and evenness of species in each phytoplankton community, while the continuous (differential) entropy gives a measure of the relative spread of the species' functional traits. The realized functional diversity (continuous entropy) and the effective richness (discrete entropy) display the same seasonality for the highest diversity simulation (not shown). However, for the lowest diversity simulation although the effective richness is maximum (16 species), the functional diversity is minimum (zero) because all the phytoplankton species are ecologically equivalent and therefore there is no spread in the species' traits; which also implies that there is no seasonal pattern in either measure of diversity.

4. Results

The model simulates the seasonal dynamics of open ocean mid latitudes using a 1D (depth-resolved) setup (see Fig. 3). Solar radiation increases from winter (December through February) to summer (June through August), which leads to an increase of sea surface temperature, stratification and shallowing of the mixing layer depth, and a decrease of turbulent diffusion. The combination of solar radiation, ocean temperature and vertical mixing controls the seasonal dynamics of community-level primary production, which we show for the marine phytoplankton community with highest functional diversity (see Fig. 3 – bottom panel). The annual peak of strongest turbulent diffusion during late winter brings nutrients to the surface and disrupt predator–prey coupling, fueling the phytoplankton spring (March through May) bloom when solar radiation starts to rise (Sverdrup, 1953; Behrenfeld and Boss, 2014). The shallow mixing layer and weaker turbulent diffusion

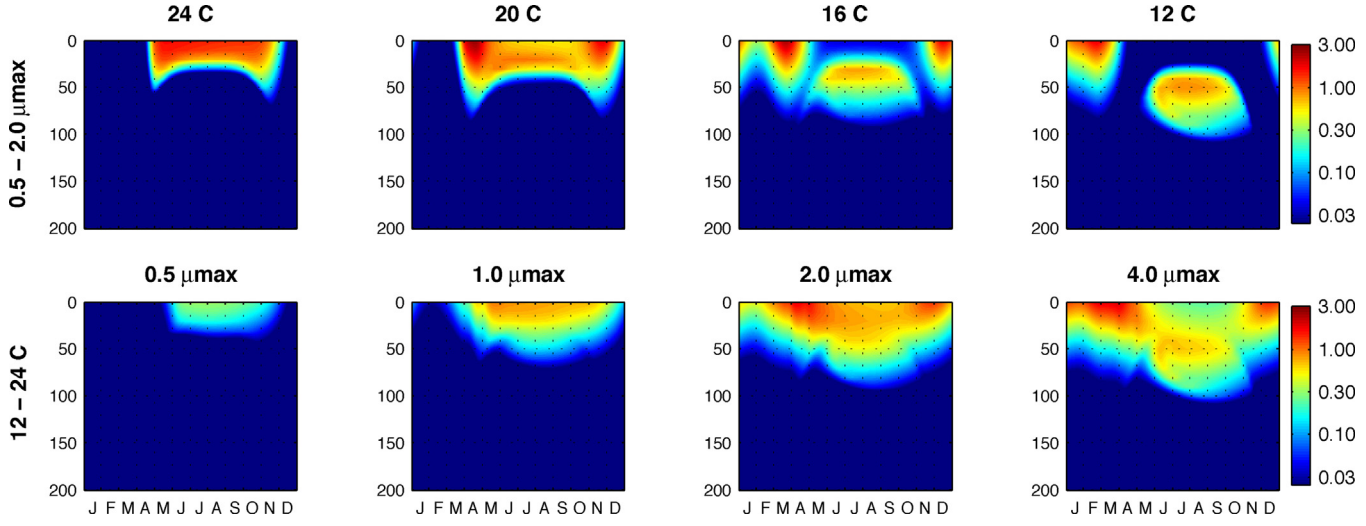

Fig. 4. Seasonal community-level primary production (mmol C m^{-3} d^{-1}) after grouping the species according to their thermal preference (given by their temperature optima) and uptake strategy (given by their maximum growth rate). The upper panels show the segregation of thermal niches that result solely from changes in ecological fitness due to environmental filtering (i.e. for a given thermal niche, all uptake strategies are present in the community). The lower panels show the segregation of nutrient niches that result solely from changes in ecological fitness due to resource competition (i.e. for a given uptake strategy, all thermal niches are present in the community). Environmental filtering leads to species asynchrony by confining the species to the thermal range where they can grow (and are filtered out elsewhere). Resource competition leads to species asynchrony by confining the species to the nutrient concentration range where they are superior competitors (and are competitive excluded elsewhere).

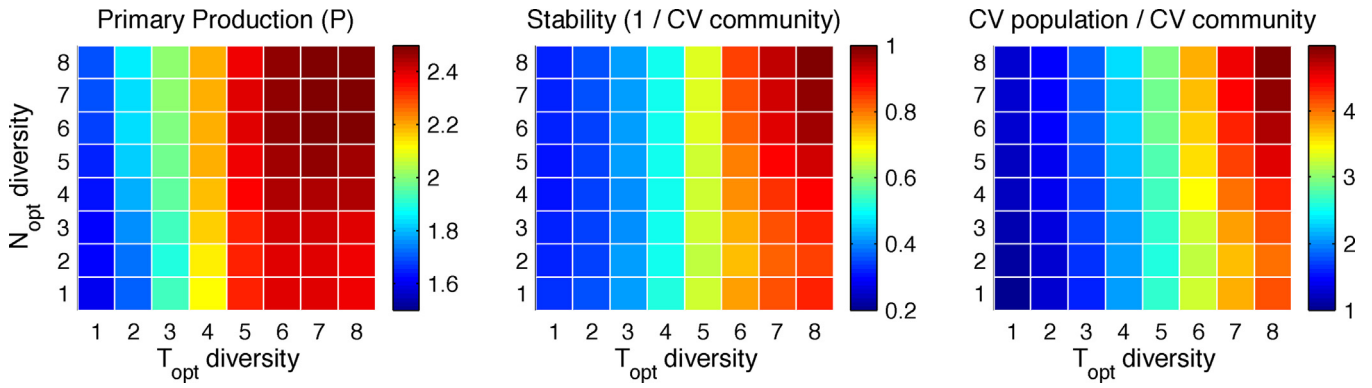

Fig. 5. Phytoplankton annual community-level primary production (mmol C m^{-3} d^{-1}), its temporal stability seasonal cycle (inverse of the coefficient of variation normalized by its maximum value; n.d.), and the ratio of temporal variability (CV) at the population-level over the community-level (n.d.) as a function of the diversity in thermal preferences (horizontal axis) and the diversity in nutrient uptake strategies (vertical axis). This figure gives the median values resulting from the 1024 simulations that were performed (see Figs. S3 and S4). Increasing the diversity of thermal preferences of the phytoplankton community (horizontal axis) leads to a strong increase in the community-level production, its temporal stability, and to the stabilization of aggregate community-level production respect to population-level production. Increasing the diversity of uptake strategies of the phytoplankton community (vertical axis) leads to a weaker increase in the community-level production, its temporal stability, and to a weaker stabilization of aggregate community-level production respect to population-level production.

during summer leads to a minima in phytoplankton production because nutrients are scarce due to vertical sinking of detritus particles outside the euphotic layer before they can be fully remineralized. A weaker secondary peak in phytoplankton production happens during autumn (September through November) when a seasonal breaking of the strong summer thermocline by turbulent diffusion brings nutrients back to the surface when solar radiation is still high enough to sustain primary production before winter comes and light limitation becomes too severe for phytoplankton to grow. Although community-level primary production for the highest functional diversity displays a smooth seasonal variability, the individual population dynamics varies considerably as each species occupies a particular (N_{opt}, T_{opt}) niche (see Fig. S2 in Supplementary Material).

By grouping the species according to either their thermal optima or uptake strategy we can isolate the segregation of niches that occur both along a temporal gradient of temperature (thermal niches) and along a temporal gradient of resource concentration (nutrient niches) (see Fig. 4). Species asynchrony along the temperature and nutrient gradients are the result of the interspecies competitive interactions and ecological fitness. The change in species fitness along the temperature gradient is due to environmental filtering of the different thermal preferences. The change in species fitness along the nutrient gradient is due to the resource competitive ability of the different uptake strategies. Yet, resource competition also occurs among species with different temperature optima if their thermal niches overlap, although this does not alter their intrinsic T_{opt}. However, it can alter the width of their response curve through niche contraction and therefore their location along the temperature gradient. Both fundamental niche differences and resource competition thus act simultaneously when species differ in their nutrient uptake strategy and thermal optimum. For the highest functional diversity simulation, each local (depth, time) phytoplankton community contains a subset of the total integrated species richness over time due to local selection and dominance of the most efficient strategies. The annually-averaged phytoplankton community contains all the species that were locally successful at some point through the year, and their observed distribution can be approximated by a gaussian probability density function pdf(N_{opt}, T_{opt}) (see Section 3). The exponential of the differential (i.e. continuous) entropy of the probability density function gives a measure of the realized functional diversity of the annual community, while the exponential of the Shannon (i.e. discrete) entropy gives a measure of its effective richness (see Fig. 6).

The impact of functional diversity on ecosystem production and stability therefore depends on the type of functional diversity we are evaluating: uptake strategy versus temperature preference. Higher functional diversity of temperature optima leads to a higher and more stable community-level production than lower diversity of temperature optima (see Fig. 5). This happens for all the combinations of the lowest functional diversity of temperature optima (see Figs. S3 and S4 in Supplementary Material). On the other hand, varying the diversity of nutrient uptake strategies has a weaker effect on both production and stability (see Fig. 5). When the lowest diversity of resource uptake strategies corresponds to a community with all species following an opportunist strategy, the community-level production and its stability is almost indistinguishable from that of a community with all resource uptake strategies present (i.e. from gleaner to opportunists) (see Figs. S3 and S4 in Supplementary Material). Therefore even though the presence of several uptake strategies should theoretically lead to a higher and more stable total community-level production through temporal selection and dominance of the most efficient strategy, in practice this positive influence of a higher diversity of uptake strategies is small. This contrasts with the strong positive influence that a higher diversity of temperature optima has on the community-level production and its temporal stability.

Increasing the potential diversity of thermal and/or uptake strategies preferences of the phytoplankton community leads to a linear increase of the realized functional diversity while the effective richness remains rather constant and close to its maximum value (see Fig. 6). Higher diversity of thermal preferences has a "direct" positive effect on ecosystem functioning on a seasonal basis because it leads to *niche complementarity* of the species, which allows covering the whole temporal gradient in temperature. Otherwise some seasons of the year would be void of any phytoplankton species, leading to suboptimal use of the nutrients and higher volatility of community-level production. This direct positive effect leads to a strong increase in the median value of primary production and its stability with T_{opt} diversity, and also to a similar increase of both the minimum and maximum values of the distribution (see Fig. 7). Covering the temporal gradient of nutrient concentration, on the other hand, does not require a diversity of uptake strategies because any strategy can do so. Yet, a higher diversity of uptake strategies still has a positive "indirect" influence

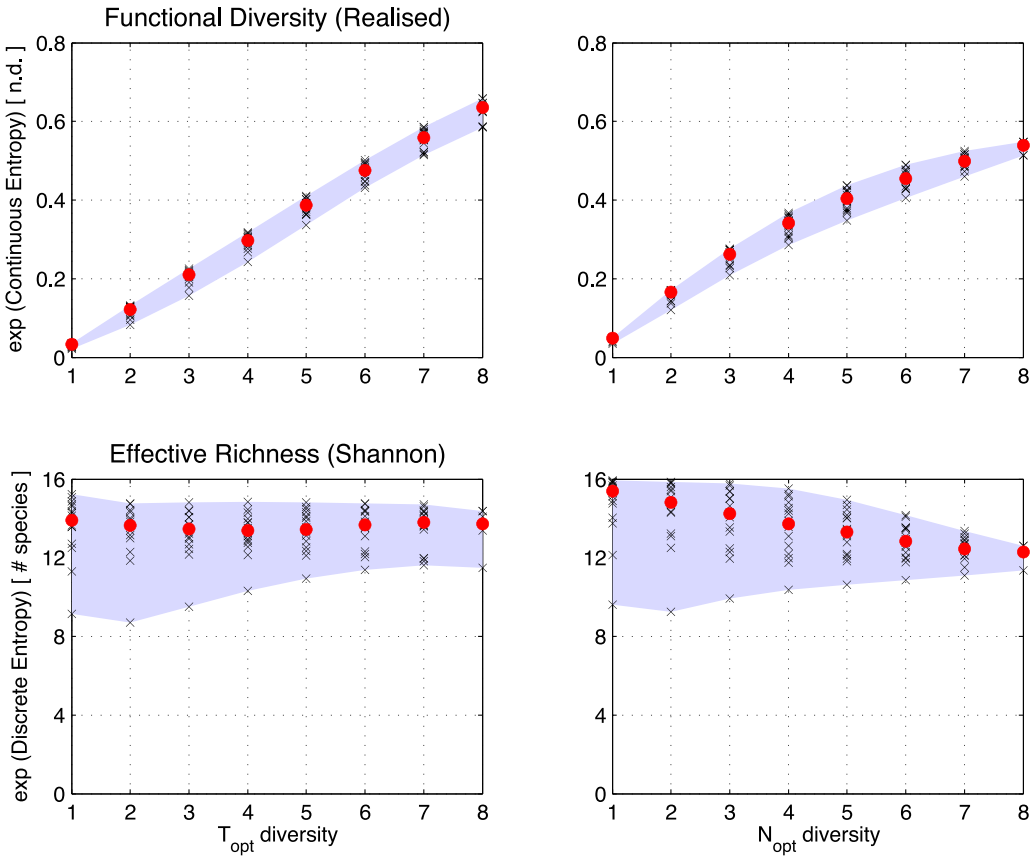

Fig. 6. Functional diversity (exponential of the differential entropy of the continuous probability density function pdf(N_{opt}, T_{opt}), normalized by its maximum value; n.d.) and effective species richness (exponential of the Shannon diversity index; # species) for the annually-averaged phytoplankton community as a function of the diversity in thermal preferences (left panels) and the diversity in nutrient uptake strategies (right panels). This figure gives the distribution of values resulting from the 1024 simulations that were performed. The red dots correspond to the median value of the distribution. The gray shaded area spans from the minimum to the maximum value of the distribution. Increasing the diversity of thermal and/or uptake strategies preferences of the phytoplankton community leads to a strong increase in the median, minimum and maximum value of the functional diversity while the effective richness remains constant and close its maximum value. (For interpretation of the references to colour in this figure legend, the reader is referred to the web version of this article.)

on ecosystem functioning through a *sampling probability* effect: the more uptake strategies are potentially available, the higher the chance of sampling a faster-growing opportunist strategy (Tilman et al., 1997). This indirect positive effect leads to a strong increase in the minimum value of production and its stability with N_{opt} diversity, but to a weak increase of the median values of the distribution, and has no effect whatsoever on the maximum values of the distribution (see Fig. 7).

5. Discussion

Community assembly theory suggest that the two main processes that determine the distribution of species are ecological fitness by resource competition ability and environmental filtering (Cornwell et al., 2006; Kraft et al., 2015). Priority effects such as species invasion order are suggested to be of minor importance for phytoplankton (i.e. being the first species to invade does not guarantee ecological success) (Robinson and Edgemon, 1988). Invasion rate can, however, alter species composition due to transient dynamics sustained by oceanic dispersal (Robinson and Edgemon, 1988; Clayton et al., 2013; Levy et al., 2014). Environmental filtering refers to the abiotic factors that prevent the survival of species in a particular environment in the absence of biotic interactions, while competitive exclusion refers to the biotic interactions that prevent the survival of species in a particular environment. Environmental filtering occurs when a species arrives at a focal site but fails to survive even in the absence of neighbours; competitive exclusion occurs when a species arrives and can persist in the absence of neighbours but not in their presence (Kraft et al., 2015). The interplay of competition- and filtering-driven fitness leads to the *ecological selection* of species, a concept that refers to changes in dominance and species composition due to survival selection on ecological time-scales driven by differences in species traits (Loreau and Hector, 2001; Litchman et al., 2015). The rate of competitive exclusion is slower for species with similar fitness (Kraft et al., 2015), which has significant implications for the coexistence of phytoplankton species in the ocean (Barton et al., 2010).

Phytoplankton species have been described to fill distinct ecological niches of temperature-, light-, and nutrient-optima (Johnson et al., 2006; Irwin et al., 2015) leading to niche partitioning along environmental gradients, which has been modelled mechanistically (Follows et al., 2007). Our simulations also show that a diversity of uptake strategies leads to species segregation along the resource concentration gradient, while a diversity of thermal preferences leads to species segregation along the temperature gradient (Fig. 4). The best adapted species to each particular environment or ecological niche tend to dominate the community (Fig. S2 in Supplementary Material). Therefore, temporal selection and dominance of ecologically superior phytoplankton species is expected to affect the average production and stability of a community of primary producers over a seasonal cycle that generates contrasting environmental conditions. More diverse communities

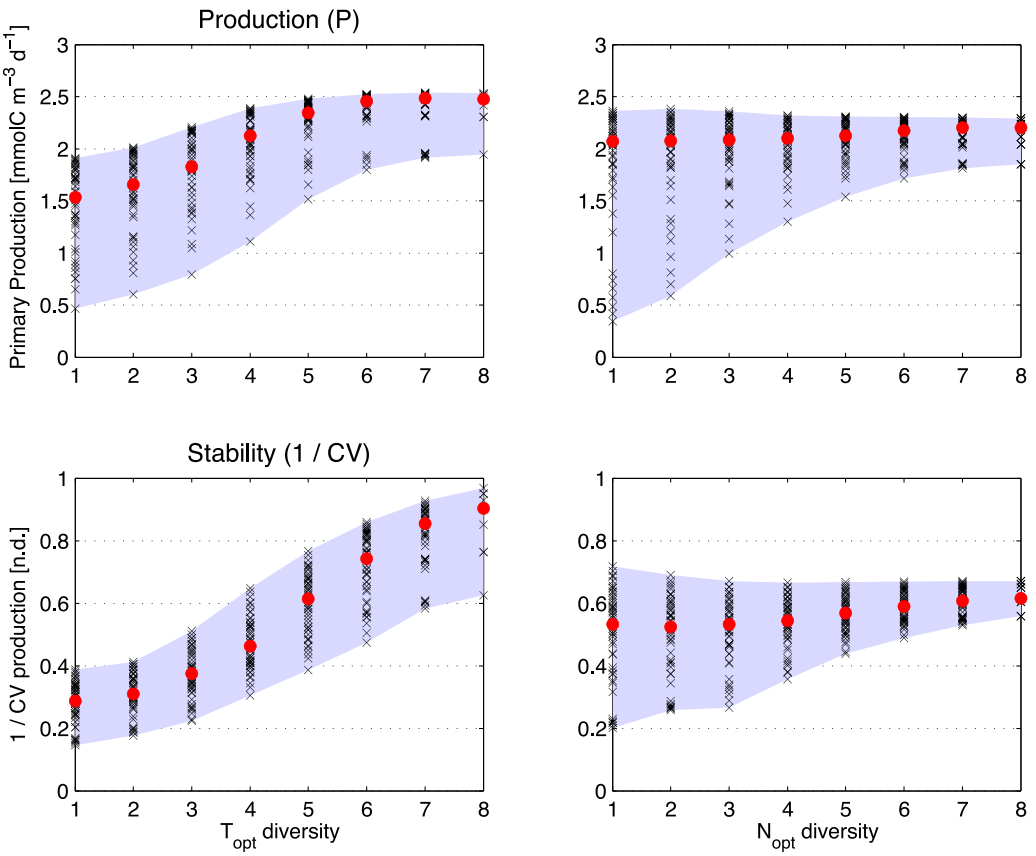

Fig. 7. Phytoplankton annual average community-level primary production (mmol C m^{-3} d^{-1}) and its temporal stability (inverse of the coefficient of variation normalized by its maximum value; n.d.) as a function of the diversity in thermal preferences (left panels) and the diversity in nutrient uptake strategies (right panels). This figure gives the distribution of values resulting from the 1024 simulations that were performed (see Figs. S3 and S4 in Supplementary Material). The red dots correspond to the median value of the distribution. The gray shaded area spans from the minimum to the maximum value of the distribution. Increasing the diversity of thermal preferences of the phytoplankton community leads to a strong increase in the median, minimum and maximum value of the community-level production and its temporal stability over a seasonal cycle. Increasing the diversity of uptake strategies of the phytoplankton community leads to a strong increase of only the minimum value of the community-level production and its temporal stability over a seasonal cycle, to a weak increase of the median value, and has no effect on the maximum values of the distribution. (For interpretation of the references to colour in this figure legend, the reader is referred to the web version of this article.)

from a functional point of view should theoretically be more capable of coping and taking advantage of this environmental variability than less diverse communities (Yachi and Loreau, 1999). More functional roles, however, may help sustain ecosystem processes under variable environmental conditions in the long run at the expenses of decreasing ecosystem performance locally (Ulanowicz et al., 2009). This has been suggested in the context of information theory (IF) as a competitive balance between "effective performance" and unutilized "reserve capacity" of any complex system based on flow networks, such as ecosystem foodwebs (Zorach and Ulanowicz, 2003). Basically, higher diversity is regarded as a way to store *potential* ecosystem functioning by paying the price of losing ecosystem performance locally. This view has led to the suggestion that ecosystems have a domain termed "window of vitality" that delimit a region of network complexity for which the ecosystem functions in the most sustainable way by optimizing this balance between opposite forces (Zorach and Ulanowicz, 2003; Ulanowicz et al., 2009).

Differences in species fundamental niches may lead to differences in realized temporal niches because the species will thus respond asynchronously to changes in the environmental conditions (Loreau, 2010). This temporal asynchrony in species environmental responses is the basis for functional compensation among competing species and explains their co-existence under non-equilibrium (e.g. seasonal) environmental conditions (Loreau, 2010; Dutkiewicz et al., 2009). Functional compensation is in turn the basis for the suggested insurance that biodiversity provides to ecosystem functioning (Yachi and Loreau, 1999). When species respond asynchronously, the average community-level production over a seasonal cycle should be expected to be higher (enhancement effect) and less variable (buffering effect) than when species respond synchronously (Yachi and Loreau, 1999). The enhancement effect of biodiversity results from transient selection and dominance of the most productive species, while the buffering effect results from compensatory dynamics (Loreau, 2010). Furthermore, having a high functionally diverse community has been suggested to lead to lower variability (high stability) of community-level production, while leading to higher variability (low stability) of the individual populations (Loreau, 2010). Our results do show that phytoplankton functional diversity increases the ratio of population- over community-level temporal variability of primary production (see Fig. 5). This reconciles early theoretical works that suggested that diversity should lead to ecosystem instability (Hutchinson, 1961; May, 1974; Tilman, 1982) with observations in the field that suggest otherwise (Tilman et al., 2006).

Are functionally-rich ecosystems more capable of both buffering environmental variability (increase stability) and enhancing ecosystem functioning (increase production) than functional-poor ecosystems? Our results suggest they do, yet the strength of the

relationship between diversity and ecosystem functioning may depend critically on the type of niche and functional diversity we are evaluating. Functional diversity along a climatic gradient such as temperature, for which species have *distinct niches* subject to environmental filtering, does lead to higher community-level production and temporal stability. A community composed by species that differ in their thermal optima will display functional compensation through time by which there is always at least one species that finds the current environmental conditions optimal for growth, while the rest of species grow sub-optimally due to environmental filtering. Thus, the community as a whole will be able to use the resources over a seasonal cycle more efficiently than a diversity-poor community composed of species that only survive during a short temporal window (only winter or only summer). Therefore, ecological selection of complementary species mediated by environmental filtering along a thermal gradient has a strong positive effect on ecosystem productivity and stability.

On the other hand, functional diversity along a resource gradient such as nutrients for which species have *shared niches*, lead to a weaker positive effect of diversity on community-level primary productivity and stability. A phytoplankton community composed of species that differ in their nutrient uptake strategy will also display functional compensation through time because there is always at least one dominant species that finds the current environmental conditions optimal for growth, at the expense of other species not being at their optimal nutrient concentration. Thus, although one would expect that in theory a community composed of species that cover the whole range of uptake strategies should lead to a higher productivity over a seasonal cycle by optimizing resource uptake, our results suggest that the enhancement is small. As long as an opportunist strategy is present in the phytoplankton community, the diversity of uptake strategies does not have a significant impact. Thus, ecological selection mediated by resource competition ability along a gradient of nutrient concentration has a weak positive effect on ecosystem productivity and stability.

An additional distinction between nutrient and temperature niches is the presence of a feedback between nutrients and phytoplankton dynamics. That is, nutrient concentrations are consumed and therefore affected by phytoplankton dynamics while ambient temperature is mostly unaffected by phytoplankton biomass (but see (Manizza, 2006)). This feedback combined with detritus sinking has a tendency to favour gleaner species during summer. The onset of the spring bloom is, however, independent of this feedback since it is controlled by vertical supply from turbulent diffusion. Thus, the nutrient concentration in the euphotic layer fluctuates seasonally as a consequence of the following processes: (i) nutrient supply (independent of biomass dynamics); (ii) primary production and vertical export by sinking particles (which depends on biomass dynamics). This makes the dynamics of phytoplankton relatively more complex along the nutrient axis than along the temperature axis. However, this increased dynamical complexity does not translate to a larger role of the diversity in uptake strategies for ecosystem functioning. Thus, we can safely conclude that nutrient feedback has a minor role in the observed difference between temperature and nutrient niches for primary production.

6. Limitations and generality

Our study measures the effect of phytoplankton functional diversity on ecosystem-level productivity and stability at seasonal time-scales, which provides large although low-frequency environmental variability. The focus was placed on community-level primary production and its stability because phytoplankton is at the base of the trophic foodweb. Marine ecosystems are generally at seasonal steady-state (i.e. annual mass balance). However, functional diversity can also affect ecosystem functioning at shorter time-scales closer to the generation times of planktonic organisms being subject to high-frequency perturbations (Smith et al., 2016). Our numerical experimental design is relatively specific; it evaluates the effect of phytoplankton diversity on ecosystem functioning along only two environmental gradients: nutrient concentration and ocean temperature. Real ecosystems have, however, many environmental axes and therefore the niche space can be huge and possibly n-dimensional. Phytoplankton species can compete for several essential nutrients (C, N, P, etc.); be subject to environmental filtering by solar radiation, pH, or some other climatic metric; may have different strategies for intracellular storage of nutrients; may have different defense strategies; etc. However, exploring high-dimensional niche spaces is probably beyond the means of simple numerical simulations. Exploring extensively our 2-dimensional niche space already required over one thousand simulations. Higher food web trophic levels will add another level of complexity. Yet our results may be generalized to many different environmental gradients. The key aspect of our study is: either the fundamental niche (i.e. in the absence of species interactions) along a given environmental gradient is "closed-ended" or it is "open-ended". The diversity of closed fundamental niches has a stronger effect on ecosystem functioning than the diversity of open fundamental niches. This conclusion should hold for any environmental gradient that falls into any of these two categories.

7. Conclusion

Functional diversity positively affects average community-level production and its temporal stability over a seasonal cycle. This effect can be either strong when there is a diversity of temperature preferences, or weak when there is a diversity of uptake strategies. Temperature niches are closed-ended due to environmental filtering, while nutrient niches only become closed by resource competition. Thus, having a diversity of thermal preferences allows a larger coverage of the range of temperature values. On the other hand, having a diversity of uptake strategies is not necessary to cover the whole range of nutrient concentration. The concept of *thermal niche* and *nutrient niche* are therefore quite different and care should be taken when making generic statements about the role of biodiversity on ecosystem functioning through species functional compensation and asynchrony of their responses to the environmental conditions. Both environmental filtering and resource competition can lead to functional compensation and asynchrony of individual populations. However, the diversity of environmental filtering niches (e.g. thermal optima) affects community-level production and stability in a much larger degree than the diversity of resource competition niches (e.g. nutrient optima).

Authors' contributions

S.M.V.: designed the initial study. Conducted model simulations. Wrote first draft of the manuscript. P.C.: provided feedback on the study design. Contributed to data analysis and interpretation of results. S.D.: provided feedback on the study design. Contributed to data analysis and interpretation of results. M.L.: provided critically important intellectual content. Contributed to the interpretation of results. J.M.M.: provided critically important intellectual content. Contributed to the interpretation of results. All authors discussed the results, reviewed the manuscript, and contributed to its subsequent revisions.

Conflict of interest

The authors declare no competing financial interests.

Acknowledgements

We thank Jim P. Grover and one anonymous reviewer for their constructive review. This work was funded by national research grants CGL2013-41256-P (MARES) and CTM2014-54926-R (SUAVE) from the Spanish government. S.M.V. and P.C. are supported by «Ramon y Cajal» (RyC) contracts from the Spanish government. S.D. was supported by NSF (grant 1434007) from the United States government. M.L. and J.M.M. are supported by the French Laboratory of Excellence project «TULIP» (ANR-10-LABX-41; ANR-11-IDEX-0002-02). M.L. was also supported by the BIOSTASES Advanced Grant, funded by the European Research Council under the European Union's Horizon 2020 research and innovation programme (grant agreement No 666971) and J.M.M. by the Region Midi- Pyrenees project (CNRS 121090).

Appendix A. Ecosystem model equations

A.1 Ecosystem model equations

$$\frac{\partial P_j}{\partial t} = F_{P_j} - E_{P_j} - G_{P_j} - M_{P_j} + \nabla_z(\kappa \nabla_z P_j) \tag{1}$$

$$\frac{\partial Z_j}{\partial t} = F_{Z_j} - E_{Z_j} - G_{Z_j} - M_{Z_j} + \nabla_z(\kappa \nabla_z Z_j) \tag{2}$$

$$\begin{aligned}\frac{\partial \mathrm{NO_3}}{\partial t} &= -F_P^{\mathrm{NO_3}} \\ &+\varepsilon_{(P\rightarrow \mathrm{NO_3})}E_P \\ &+\varepsilon_{(Z\rightarrow \mathrm{NO_3})}E_Z \\ &+\Omega_{(P\rightarrow \mathrm{NO_3})}M_P \\ &+\Omega_{(Z\rightarrow \mathrm{NO_3})}M_Z \\ &+\delta_{(PON\rightarrow \mathrm{NO_3})}M_{\mathrm{PON}} \\ &+\delta_{(DON\rightarrow \mathrm{NO_3})}M_{DON} \\ &+\delta_{(\mathrm{NH_4}\rightarrow \mathrm{NO_3})}M_{\mathrm{NH_4}} \\ &+\nabla_z(\kappa \nabla_z \mathrm{NO_3})\end{aligned} \tag{3}$$

$$\begin{aligned}\frac{\partial \mathrm{NH_4}}{\partial t} &= -F_P^{\mathrm{NH_4}} - M_{\mathrm{NH_4}} \\ &+\varepsilon_{(P\rightarrow \mathrm{NH_4})}E_P + \varepsilon_{(Z\rightarrow \mathrm{NH_4})}E_Z \\ &+\Omega_{(P\rightarrow \mathrm{NH_4})}M_P + \Omega_{(Z\rightarrow \mathrm{NH_4})}M_Z \\ &+\delta_{(PON\rightarrow \mathrm{NH_4})}M_{\mathrm{PON}} + \delta_{(DON\rightarrow \mathrm{NH_4})}M_{DON} \\ &+\nabla_z(\kappa \nabla_z \mathrm{NH_4})\end{aligned} \tag{4}$$

$$\begin{aligned}\frac{\partial DON}{\partial t} &= -M_{DON} \\ &+\varepsilon_{(P\rightarrow DON)}E_P + \varepsilon_{(Z\rightarrow DON)}E_Z \\ &+\Omega_{(P\rightarrow DON)}M_P + \Omega_{(Z\rightarrow DON)}M_Z \\ &+\delta_{(PON\rightarrow DON)}M_{\mathrm{PON}} \\ &+\nabla_z(\kappa \nabla_z DON)\end{aligned} \tag{5}$$

$$\begin{aligned}\frac{\partial PON}{\partial t} &= -M_{\mathrm{PON}} \\ &+\varepsilon_{(P\rightarrow PON)}E_P + \varepsilon_{(Z\rightarrow PON)}E_Z \\ &+\Omega_{(P\rightarrow PON)}M_P + \Omega_{(Z\rightarrow PON)}M_Z \\ &+\nabla_z(\kappa \nabla_z PON) + \omega \nabla_z PON\end{aligned} \tag{6}$$

A.2 Phytoplankton production

$$F_{P_j} = F_{P_j}^{\mathrm{NO_3}} + F_{P_j}^{\mathrm{NH_4}} \tag{7}$$

$$F_{P_j}^{\mathrm{NO_3}} = \mu_{P_j}^{\max}(Q_{P_j}^{\mathrm{NO_3}} Q_{P_j}^{\mathrm{SST}} Q^{\mathrm{PAR}})P_j \tag{8}$$

$$F_{P_j}^{\mathrm{NH_4}} = \mu_{P_j}^{\max}(Q_{P_j}^{\mathrm{NH_4}} Q_{P_j}^{SST} Q^{PAR})P_j \tag{9}$$

$$F_P^{\mathrm{NO_3}} = \sum_j F_{P_j}^{\mathrm{NO_3}} \tag{10}$$

$$F_P^{\mathrm{NH_4}} = \sum_j F_{P_j}^{\mathrm{NH_4}} \tag{11}$$

$$F_P = \sum_j F_{P_j} \tag{12}$$

$$Q_{P_j}^{\mathrm{DIN}} = Q_{P_j}^{\mathrm{NO_3}} + Q_{P_j}^{\mathrm{NH_4}} \leq 1 \tag{13}$$

$$Q_{P_j}^{\mathrm{NH_4}} = \left(\frac{\mathrm{NH_4}}{K_{P_j}^{\mathrm{DIN}} + \mathrm{NH_4}}\right) \tag{14}$$

$$Q_{P_j}^{\mathrm{NO_3}} = \left(\frac{\mathrm{NO_3}}{K_{P_j}^{\mathrm{DIN}} + \mathrm{NO_3}}\right)(1 - Q_{P_j}^{\mathrm{NH_4}}) \tag{15}$$

$$Q^{PAR} = \left(\frac{I}{I_{opt}}\right)\exp\left(1 - \left(\frac{I}{I_{opt}}\right)\right) \leq 1 \tag{16}$$

$$Q_{P_j}^{SST} = 2(\mathrm{pdf}\,(x)\ \mathrm{cdf}\,(z)) \leq 1 \tag{17}$$

$$\mathrm{pdf}\,(x) = \left(\frac{1}{\sqrt{2\pi}}\right)\exp(-x^2/2) \tag{18}$$

$$\mathrm{cdf}\,(z) = \left(\frac{1}{2}\right)(1.0 + \ \mathrm{erf}\,(z)) \tag{19}$$

$$\mathrm{erf}\,(z) \approx \tanh(z) = \frac{(\exp(z) - \exp(-z))}{(\exp(z) + \exp(-z))} \tag{20}$$

$$z = \sqrt{\pi}\log(2)\left(\frac{x\rho_T}{\sqrt{2}}\right) \tag{21}$$

$$x = \frac{T - T_{opt}}{\sigma_T} \tag{22}$$

$$I = I_0 \exp\left(-\int_0^z (k_w + k_p \sum_j P_j)dz\right) \tag{23}$$

A.3 Zooplankton production (prey$_i$, predator$_j$)

$$Q_{Z_j} = \sum_i Q_{Z_j}^{P_i} + \sum_i Q_{Z_j}^{Z_i} = Q_{Z_j}^{tot} \leq 1 \tag{24}$$

$$Q_{Z_j}^{P_i} = \frac{\phi_{ij} P_i^{\alpha}}{(\sum_k \phi_{kj} P_k^{\alpha} + \sum_k \varphi_{kj} Z_k^{\alpha})} Q_{Z_j}^{tot} \tag{25}$$

$$Q_{Z_j}^{Z_i} = \frac{\varphi_{ij} Z_i^{\alpha}}{(\sum_k \phi_{kj} P_k^{\alpha} + \sum_k \varphi_{kj} Z_k^{\alpha})} Q_{Z_j}^{tot} \tag{26}$$

$$Q_{Z_j}^{tot} = \frac{(\sum_k \phi_{kj} P_k + \sum_k \varphi_{kj} Z_k)^{\beta}}{K_{Z_j}^{\beta} + (\sum_k \phi_{kj} P_k + \sum_k \varphi_{kj} Z_k)^{\beta}} \tag{27}$$

$$G_{P_i} = \sum_j (\mu_{Z_j}^{\max} Z_j) Q_{Z_j}^{P_i} \tag{28}$$

$$G_{Z_i} = \sum_j (\mu_{Z_j}^{\max} Z_j) Q_{Z_j}^{Z_i} \quad (29)$$

$$F_{Z_j} = (\mu_{Z_j}^{\max} Z_j) Q_{Z_j} \quad (30)$$

$$F_Z = \sum_j F_{Z_j} \quad (31)$$

A.4 Plankton exudation/excretion

$$E_{P_j} = (1 - \beta_P) F_{P_j} \quad (32)$$

$$E_{Z_j} = (1 - \beta_Z) F_{Z_j} \quad (33)$$

$$E_P = (1 - \beta_P) F_P \quad (34)$$

$$E_Z = (1 - \beta_Z) F_Z \quad (35)$$

A.5 Plankton mortality

$$M_{P_j} = \psi_P P_j \quad (36)$$

$$M_{Z_j} = \psi_Z Z_j \quad (37)$$

$$M_P = \psi_P \sum P_j \quad (38)$$

$$M_Z = \psi_Z \sum Z_j \quad (39)$$

A.6 Matter decomposition

$$M_{NH_4} = \psi_{NH_4} NH_4 \quad (40)$$

$$M_{DON} = \psi_{DON} DON \quad (41)$$

$$M_{PON} = \psi_{PON} PON \quad (42)$$

Appendix B. Supplementary data

Supplementary data associated with this article can be found, in the online version, at http://dx.doi.org/10.1016/j.ecolmodel.2017.06.020.

References

Barton, A., Dutkiewicz, S., Flierl, G., Bragg, J.G., Follows, M.J., 2010. Patterns of diversity in marine phytoplankton. Science 327, 1509–1511.

Behrenfeld, M.J., Boss, E.S., 2014. Resurrecting the ecological underpinnings of ocean plankton blooms. Annu. Rev. Mar. Sci. 6, 167–194.

Carr, M.H., Neigel, J.E., Estes, J.A., Andelman, S., Warner, R.R., Largier, J.L., 2003. Comparing marine and terrestrial ecosystems: implications for the design of coastal marine reserves. Ecol. Appl. 13 (1), S90–S107.

Cermeno, P., Lee, J.-B., Wyman, K., Schofield, O., Falkowski, P.G., 2011. Competitive dynamics in two species of marine phytoplankton under non-equilibrium conditions. Mar. Ecol. Prog. Ser. 429, 19–28.

Clayton, S., Dutkiewicz, S., Jahn, O., Follows, M.J., 2013. Dispersal, eddies, and the diversity of marine phytoplankton. Limnol. Oceanogr. Fluids Environ. 3 (1), 182–197, http://dx.doi.org/10.1215/21573689-2373515.

Cornwell, W.K., Schwilk, D.W., Ackerly, D.D., 2006. A trait-based test for habitat filtering: convex hull volume. Ecology 87 (6), 1465–1471.

Duffy, J.E., 2009. Why biodiversity is important to the functioning of realworld ecosystems. Front. Ecol. Environ. 7, 437–444.

Dutkiewicz, S., Follows, M.J., Bragg, J.G., 2009. Modeling the coupling of ocean ecology and biogeochemistry. Glob. Biogeochem. Cycles 23, 1–15.

Follows, M.J., Dutkiewicz, S., Grant, S., Chisholm, S.W., 2007. Emergent biogeography of microbial communities in a model ocean. Science 315, 1843–1846.

Grover, J.P., 1997. Resource Competition. Population and Community Biology Series. Springer.

Hector, A., Schmid, B., Beierkuhnlein, C., Caldeira, M.C., Diemer, M., Dimitrakopoulos, P.G., Finn, J.A., Freitas, H., Giller, P.S., Good, J., Harris, R., Högberg, P., Huss-Danell, K., Joshi, J., Jumpponen, A., Körner, C., Leadley, P.W., Loreau, M., Minns, A., Mulder, C.P.H., O'Donovan, G., Otway, S.J., Pereira, J.S., Prinz, A., Read, D.J., Scherer-Lorenzen, M., Schulze, E.-D., Siamantziouras, A.-S.D., Spehn, E.M., Terry, A.C., Troumbis, A.Y., Woodward, F.I., Yachi, S., Lawton, J.H., 1999. Plant diversity and productivity experiments in European grasslands. Science 286 (5442), 1123–1127 http://www.sciencemag.org/content/286/5442/1123.abstract.

Huston, M.A., DeAngelis, D.L., 1994. Competition and coexistence: the effects of resource transport and supply rates. Am. Nat. 144 (6), 954–977.

Hutchinson, G.E., 1957. Concluding remarks. Cold Spring Harbor Symp. Quant. Biol. 22 (2), 415–427.

Hutchinson, G.E., 1961. The paradox of the plankton. Am. Nat. 95 (882), 137–145.

Irwin, A.J., Finkel, Z.V., Muller-Karger, F.E., Ghinaglia, L.T., 2015. Phytoplankton adapt to changing ocean environments. Proc. Natl. Acad. Sci. U.S.A. 112 (18), 5762–5766.

Isbell, F., Gonzalez, A., Loreau, M., Cowles, J., Diaz, S., Hector, A., Mace, G.M., Wardle, D.A., O'Connor, M.I., Duffy, J.E., Turnbull, L.A., Thompson, P.L., Larigauderie, A., 2017. Linking the influence and dependence of people on biodiversity across scales. Nature 546, 65–72.

Johnson, Z.I., Zinser, E.R., Coe, A., McNulty, N.P., Woodward, E.M.S., Chisholm, S.W., 2006. Niche partitioning among prochlorococcus ecotypes along ocean-scale environmental gradients. Science 311, 1737–1740.

Kraft, N.J.B., Adler, P.B., Godoy, O., James, E.C., Fuller, S., Levine, J.M., 2015. Community assembly, coexistence and the environmental filtering metaphor. Funct. Ecol. 29 (5), 592–599.

Levy, M., Jahn, O., Dutkiewicz, S., Follows, M.J., 2014. Phytoplankton diversity and community structure affected by oceanic dispersal and mesoscale turbulence. Limnol. Oceanogr. Fluids Environ. 4 (1), 67–84, http://dx.doi.org/10.1215/21573689-2768549.

Litchman, E., Edwards, K.F., Klausmeier, C.A., 2015. Microbial resource utilization traits and trade-offs: implications for community structure, functioning, and biogeochemical impacts at present and in the future. Front. Microbiol. 6 (254), 1–10.

Loreau, M., 2010. From Populations to Ecosystems: Theoretical Foundations for a New Ecological Synthesis. Princeton University Press, Princeton, NJ.

Loreau, M., de Mazancourt, C., 2013. Biodiversity and ecosystem stability: a synthesis of underlying mechanisms. Ecol. Lett. 16, 106–115.

Loreau, M., Hector, A., 2001. Partitioning selection and complementarity in biodiversity experiments. Nature 412, 72–76.

Loreau, M., Naeem, S., Inchausti, P., 2002. Biodiversity and Ecosystem Functioning: Synthesis and Perspectives. Oxford University Press.

Manizza, M., 2006. Modelling Phytoplankton-Light Feedback and Its Ocean Biogeochemical Implications (Ph.D. thesis). University of East Anglia.

May, R.M., 1974. Stability and Complexity in Model Ecosystems. Princeton University Press, Princeton, NJ.

Meyer, J.R., Gudelj, I., Beardmore, R., 2015. Biophysical mechanisms that maintain biodiversity through trade-offs. Nat. Commun. 6 (6278), 1–7.

Naeem, S., Duffy, J.E., Zavaleta, E., 2012. The functions of biological diversity in an age of extinction. Science 336 (6087), 1401–1406.

Ptacnik, R., Solimini, A.G., an Timo Tamminen, T.A., Brettum, P., Lepistö, L., Willen, E., Rekolainen, S., 2008. Diversity predicts stability and resource use efficiency in natural phytoplankton communities. Proc. Natl. Acad. Sci. U.S.A. 105 (13), 5134–5138.

Robinson, J.V., Edgemon, M.A., 1988. An experimental evaluation of the effect of invasion history on community structure. Ecology 69 (5), 1410–1417.

Shannon, C.E., 1948. A mathematical theory of communication. Bell Syst. Techn. J. 27 (3), 379–423, http://dx.doi.org/10.1002/j.1538-7305.1948.tb01338.x.

Smayda, T.J., Reynolds, C.S., 2001. Community assembly in marine phytoplankton: application of recent models to harmful dinoflagellate blooms. J. Plankton Res. 23 (5), 447–461.

Smith, S.L., Vallina, S.M., Merico, A., 2016. Functional diversity mediates an emergent trade-off in the response of phytoplankton communities to rare versus frequent disturbances. Sci. Rep. (under revision).

Sommer, U., 1981. The role of r- and k- selection in the succession of phytoplankton in lake constance. Acta Oecol. 2 (4), 327–342.

Sommer, U., 1984. The paradox of the plankton: fluctuations of phosphorous availability maintain diversity of phytoplankton in flow-through cultures. Limnol. Oceanogr. 29 (3), 633–636.

Sommer, U., 1985. Comparison between steady state and non-steady state competition: experiments with natural phytoplankton. Limnol. Oceanogr. 30 (2), 335–346.

Sommer, U., 1986. Phytoplankton competition along a gradient of dilution rates. Oecologia 68, 503–506.

Sommer, U., 2002. Competition and Coexistence in Plankton Communities, Vol. 161 of Ecological Studies. Springer, Berlin, Germany.

Sverdrup, H.U., 1953. On conditions for the vernal blooming of phytoplankton. J. Cons. Int. Explor. Mer. 18, 287–295.

Thebault, Loreau, M., 2005. Trophic interactions and the relationship between species diversity and ecosystem stability. Am. Nat. 166 (4), E95–E114.

Tilman, D., 1982. Resource Competition and Community Structure, Vol. 17 of Monographs in Population Biology. Princeton University Press, Princeton, NJ.

Tilman, D., Lehman, C., Thomson, K.T., 1997. Plant diversity and ecosystem productivity: Theoretical considerations. Proc. Natl. Acad. Sci. U.S.A. 94, 1857–1861.

Tilman, D., Reich, P.B., Knops, J., Wedin, D., Mielke, T., Lehman, C., 2001. Diversity and productivity in a long-term grassland experiment. Science 294 (5543), 843–845 http://www.sciencemag.org/content/294/5543/843.abstract.

Tilman, D., Reich, P.B., Knops, J.M.H., 2006. Biodiversity and ecosystem stability in a decade-long grassland experiment. Nature 441, 629–632.

Ulanowicz, R.E., Goerner, S.J., Lietaer, B., Gomez, R., 2009. Quantifying sustainability: resilience, efficiency and the return of information theory. Ecol. Complex. 6, 27–36.
Vallina, S.M., Follows, M.J., Dutkiewicz, S., Montoya, J.M., Cerme no, P., Loreau, M., 2014a. Global relationship between phytoplankton diversity and productivity in the ocean. Nat. Commun. 5, 4299.
Vallina, S.M., Le Quéré, C., 2008. Preferential uptake of ammonium over nitrate in marine ecosystem models: a simple and more consistent parameterization. Ecol. Modell. 218, 393–397.
Vallina, S.M., Word, B.A., Dutkiewicz, S., Follows, M.J., 2014b. Maximal feeding with active prey-switching: a kill-the-winner functional response and its effect on global diversity and biogeography. Prog. Oceanogr. 120, 93–109.
Wisheu, I.C., 1998. How organisms partition habitats: different types of community organization can produce identical patterns. Oikos 83 (2), 246–258, URL http://www.jstor.org/stable/3546836.
Yachi, S., Loreau, M., 1999. Biodiversity and ecosystem productivity in a fluctuating environment: The insurance hypothesis. Proc. Natl. Acad. Sci. U.S.A. 96, 1463–1468.
Zorach, A.C., Ulanowicz, R.E., 2003. Quantifying the complexity of flow networks: how many roles are there? Complexity 8 (3), 68–76.

Supplementary Material

		Temperature Optimum			
		12℃	16℃	20℃	24℃
Max. growth	0.5 d^{-1}	Phy $_{01}$	Phy $_{02}$	Phy $_{03}$	Phy $_{04}$
	1.0 d^{-1}	Phy $_{05}$	Phy $_{06}$	Phy $_{07}$	Phy $_{08}$
	2.0 d^{-1}	Phy $_{09}$	Phy $_{10}$	Phy $_{11}$	Phy $_{12}$
	4.0 d^{-1}	Phy $_{13}$	Phy $_{14}$	Phy $_{15}$	Phy $_{16}$

Table S1: Phytoplankton species that compose the only community with the highest functional diversity: each of the 16 species have a different uptake strategy (given by their maximum growth rate) from resource gleaners to resource opportunists, and a different temperature preference (given by their thermal optima) from cold water to warm waters. Note that there is only one species combination for the highest diversity community but several for the lowest diversity community (see Table S2). This phytoplankton community follows a niche model.

		Temperature Optimum			
		20℃	20℃	20℃	20℃
Max. growth	2.0 d^{-1}	Phy $_{01}$	Phy $_{02}$	Phy $_{03}$	Phy $_{04}$
	2.0 d^{-1}	Phy $_{05}$	Phy $_{06}$	Phy $_{07}$	Phy $_{08}$
	2.0 d^{-1}	Phy $_{09}$	Phy $_{10}$	Phy $_{11}$	Phy $_{12}$
	2.0 d^{-1}	Phy $_{13}$	Phy $_{14}$	Phy $_{15}$	Phy $_{16}$

Table S2: Phytoplankton species that compose one of the communities with the lowest functional diversity: each of the 16 species have exactly the same uptake strategy (given by their maximum growth rate) of all being resource opportunists, and exactly the same temperature preference (given by their thermal optima) of all being warm waters species. This combination shows a community of perfectly redundant species where all have the same traits as Phy $_{11}$ selected in blue from Table 1. Selecting any other Phy$_j$ from Table 1 will lead to a different community of perfectly redundant species. Note that there are thus 16 combinations for the lowest functionally diverse community. This table only shows one of them as an example. These phytoplankton communities are all ecologically equivalent.

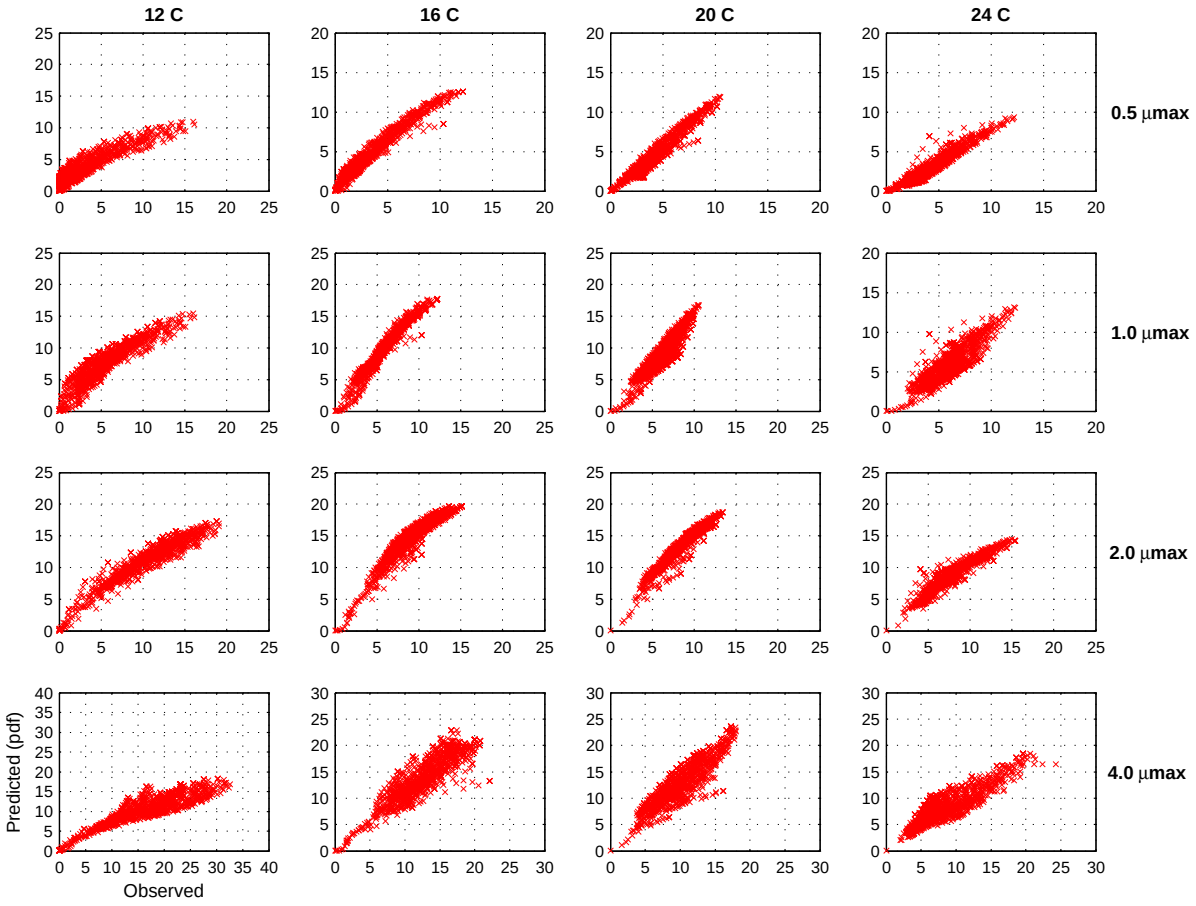

Figure S1: Biomass of each phytoplankton species as predicted by the continuous gaussian probability density function $\mathrm{pdf}(\mathrm{N_{opt}}, \mathrm{T_{opt}})$ that was fitted to the observed phytoplankton species distributions. The gaussian approximation is fairly accurate and leads to a good agreement between the observed and predicted biomass of each phytoplankton species for the 1024 simulations that were performed.

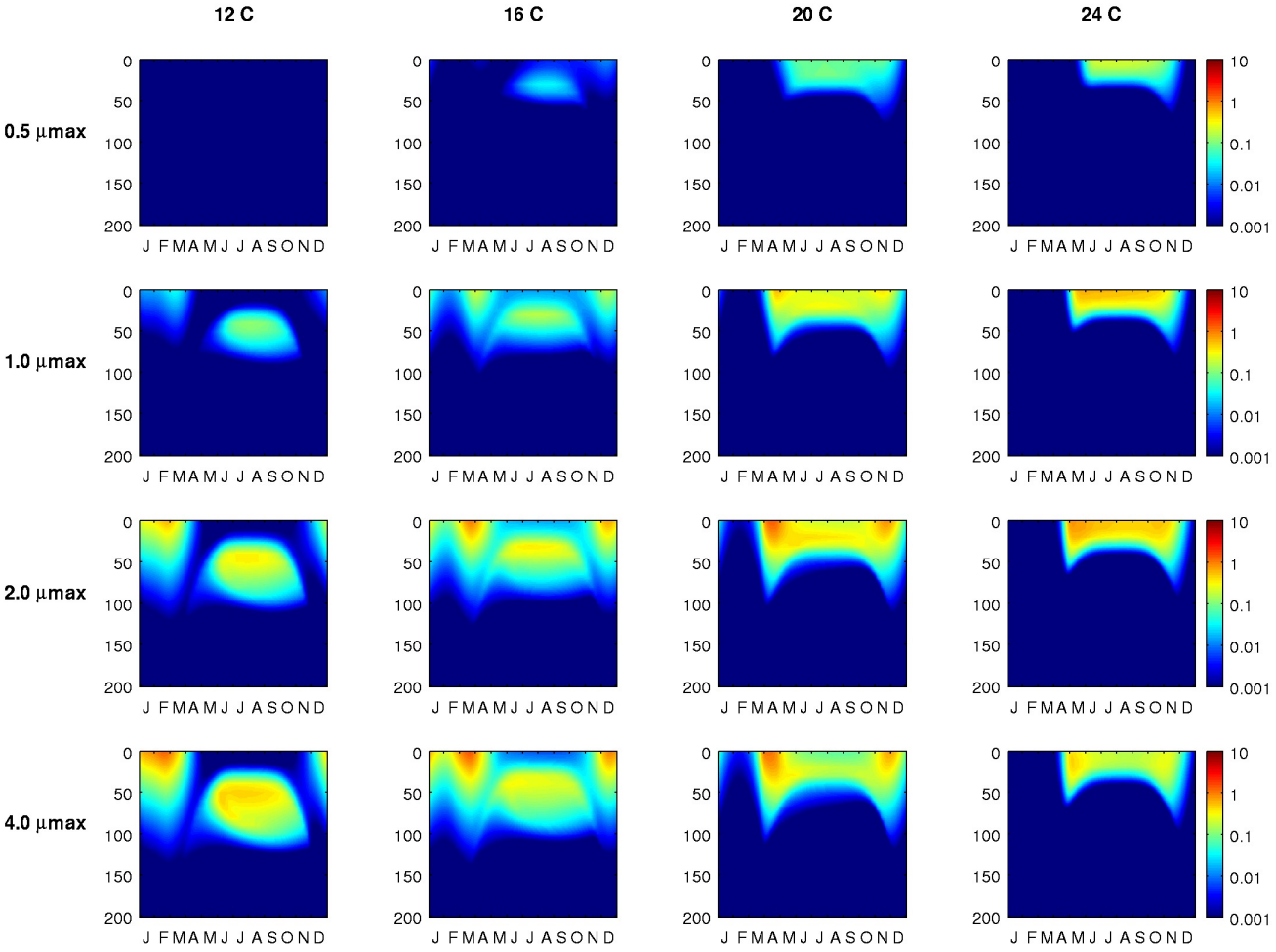

Figure S2: Seasonal production P (mmolC m^{-3} d^{-1}) of the 16 phytoplankton species for the community with the highest functional diversity, which shows their ecological niche (T_{opt}, N_{opt}) that results from their thermal preference given by their temperature optima (column-panels) and uptake strategy given by their maximum growth rate (row-panels). Environmental filtering leads to species asynchrony by confining the species to the thermal range where they can grow (and are filtered out elsewhere). Resource competition leads to species asynchrony by confining the species to the nutrient concentration range where they are superior competitors (and are competitive excluded elsewhere). Therefore each species dominate in their particular ecological niche through *ecological selection*, which is the combination of resource competition and environmental filtering acting simultaneously.

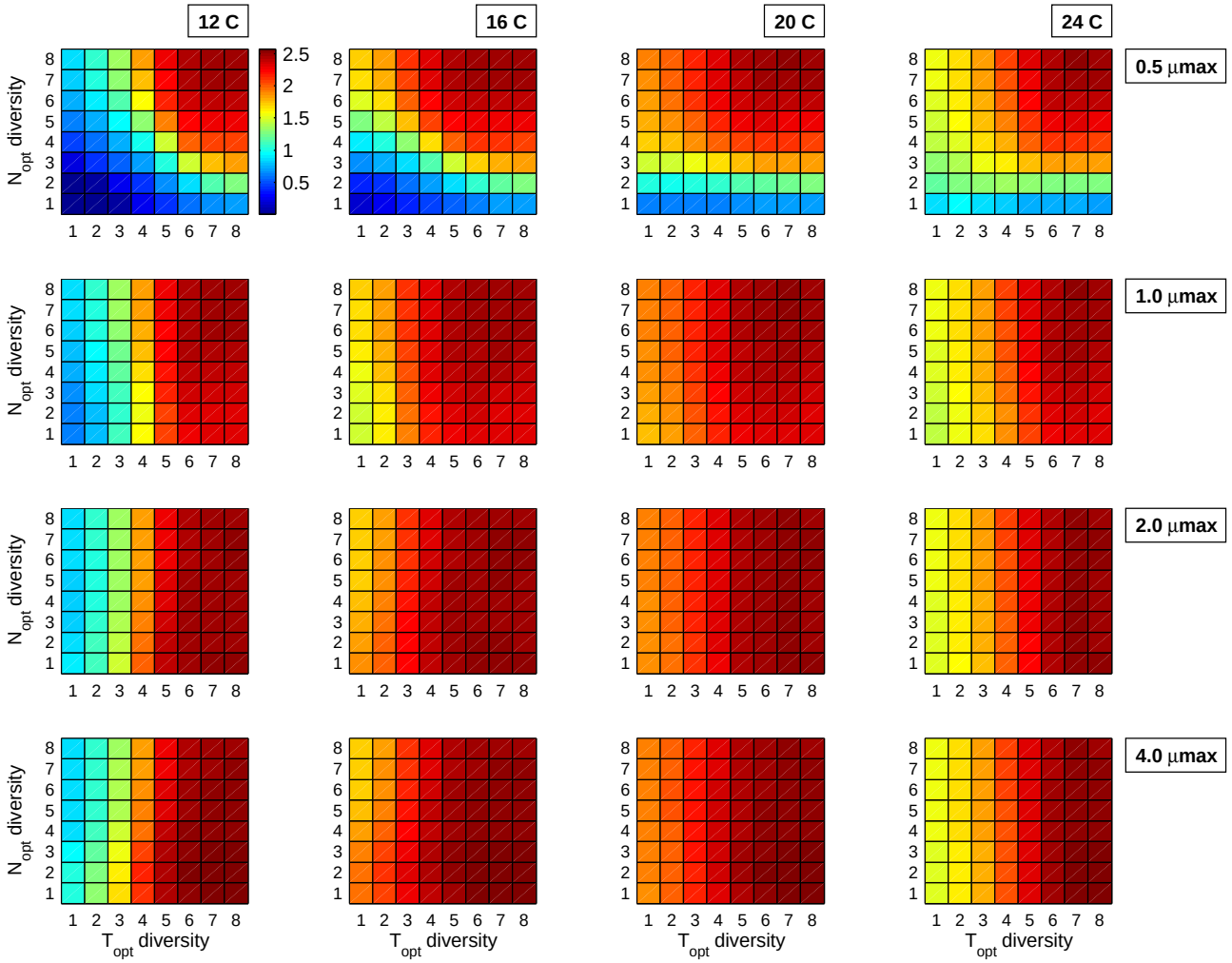

Figure S3: Phytoplankton annual average community-level primary production (mmolC m^{-3} d^{-1}) as a function of functional diversity (within each subpanel) for different combinations of phytoplankton species traits at the highest redundancy community (different subpanels). For each subpanel, the horizontal axis gives the degree of diversity in temperature preferences, while the vertical axis gives the degree of diversity in nutrient uptake strategies: functional diversity is gradually decreased from the highest functional diversity at the (8,8) square to the lowest functional diversity (perfect species redundancy) at the (1,1) square. The (8,8) inset squares for the different subpanels correspond to the same highest diversity community where phytoplankton species are covering the whole spectra of 4 uptake strategies and 4 temperature preferences. However the (1,1) inset squares for the different subpanels correspond to different lowest diversity (perfectly redundant) communities. For example, the phytoplankton species of the community for the first-row and fourth-column subpanel start as a highly diverse community covering all 4 uptake strategies and 4 temperature preferences at the (8,8) square and will gradually converge to a low diversity community of fully redundant species that have just one uptake strategy (nutrient gleaners; $\mu_{\max}$ = 0.5) and one temperature preference (warm waters; $\mathrm{T_{opt}}$ = 24 C) at the (1,1) square. Thus the four $\mu_{\max}$ and four $\mathrm{T_{opt}}$ give the one uptake strategy and one temperature preferences to where the phytoplankton species will eventually converge to become fully redundant communities at the (1,1) squares. These are the 16 combinations for the lowest functionally diverse community. Each subpanel corresponds to one of them: 4 uptake strategies (defined by the maximum growth rate; column-panels) x 4 temperature preferences (defined by the thermal optima; row-panels) = 16 ecological niches ($\mathrm{N_{opt}}$, $\mathrm{T_{opt}}$) to where all the species in the community can potentially converge to become perfectly redundant. Therefore a total of 8 x 8 x 4 x 4 = 1024 simulations where performed to cover the whole range of potential combinations of functional diversity.

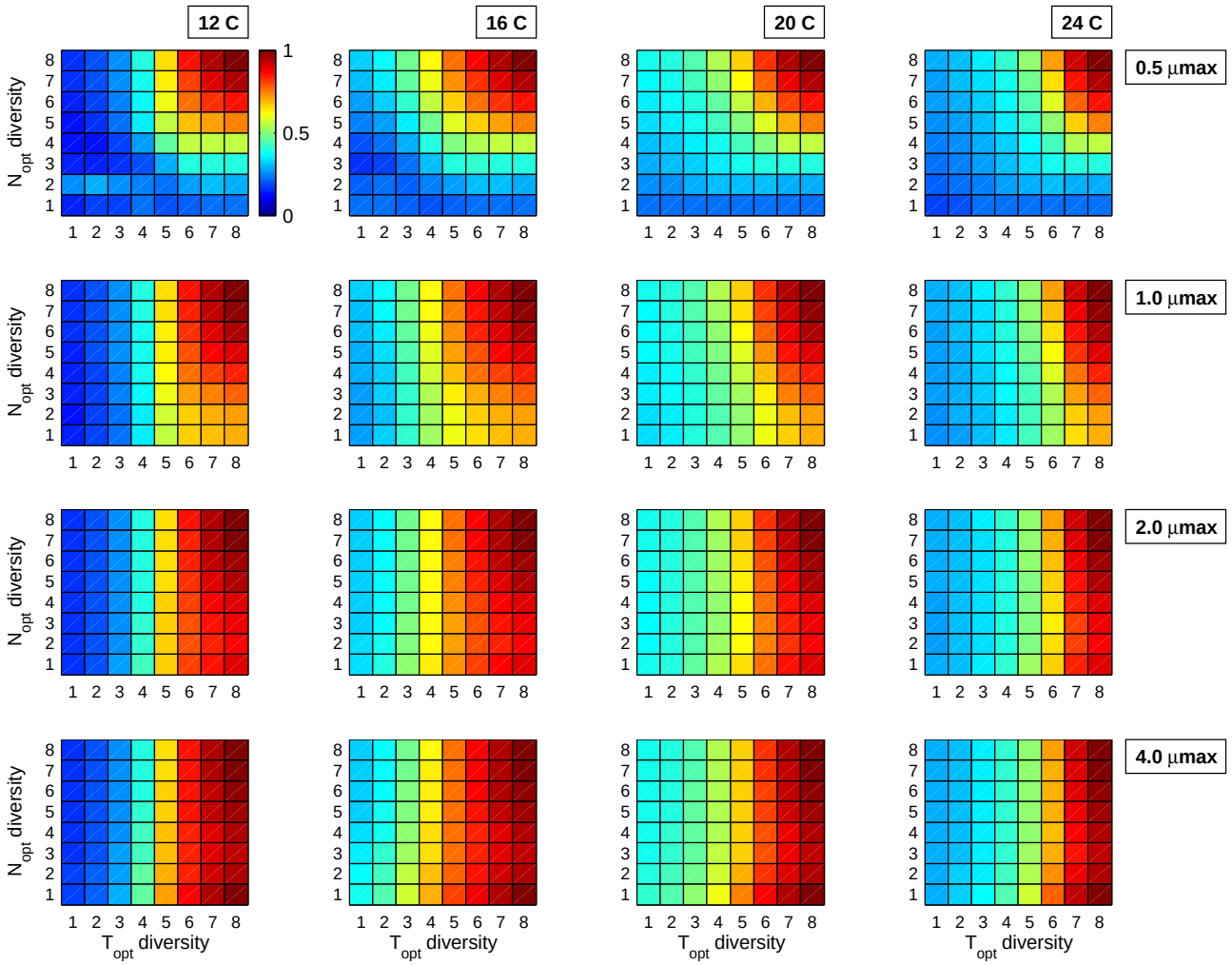

Figure S4: Temporal stability (inverse of the coefficient of variation normalized by its maximum value; n.d.) of the phytoplankton community-level primary production (mmolC m^{-3} d^{-1}) as a function of functional diversity (within each subpanel) for different combinations of phytoplankton species traits at the highest redundancy community (different subpanels). See caption of Figure S3 for more details.